MECHANICAL PROPERTIES OF Si_3N_4/SiC NANOCOMPOSITE MEASURED BY NANOINDENTATION

P. Hvizdoš, M. Kašiarová, J. Dusza, P. Šajgalík, M. Hnatko

Abstract

Contact deformation behaviour and mechanical properties of Si_3N_4/SiC nanocomposite were investigated by nanoindentation with spherical and Berkovich diamond indenters at low loads (1 – 300 mN) using depth sensing techniques. From the measurement of the tip displacement depending on the load and the tip geometry, the total and the remnant depth of penetration were found. Based on the results we were able to study elastic, yield and plastic behaviour. Using the method of partial unloading, the contact stress-strain curves, hardness, and modulus of elasticity were explored using spherical indenter tip. The values of hardness and modulus were compared to those obtained by simple loading-unloading tests made by a Berkovich indenter. The hardness values were also compared to those obtained using standard Vickers indentation.

Keywords: nanocomposite, nanoindentation, elasticity, hardness, spherical indenters

INTRODUCTION

Recently, there has been a great world-wide interest in developing and characterizing new nano-structured materials. These newly developed materials are often prepared in limited quantities and shapes unsuitable for extensive mechanical testing. The development of depth sensing indentation methods have introduced the advantage of load and depth measurement during the indentation cycle. This enables, using a simple and fast measurement, to evaluate not only hardness, for which the indentation is traditionally used, but also elastic modulus, yield behaviour, plasticity, the onset of other irreversible deformation processes such as cracking or pressure induced phase transformations, time dependent phenomena such as creep and recovery and the energy absorbed during indentation [1]. These problems can be studied on very small samples, with high spatial resolution, and non-destructively, if necessary.

The aim of the present study was to investigate some mechanical properties of a newly developed nanocomposite [2] using depth sensing indentation and, when appropriate, to compare the results with those obtained by more traditional methods.

THEORETICAL BACKGROUND

Indentation with spheres

Indentation of an infinite half space by a sphere is initially elastic, and was first considered by Hertz [3]. The elastic penetration, h_e, of a sphere (indenter) of radius R_i into a flat surface (tested material) under force F is given [4]

Pavol Hvizdoš, Monika Kašiarová, Ján Dusza, Institute of Materials Research, Slovak Academy of Sciences, Košice, Slovak Republic

Pavol Šajgalík, Milan Hnatko, Institute of Inorganic Chemistry, Slovak Academy of Sciences, Bratislava, Slovak Republic

$$h_e = (9/16)^{1/3} (F/E^*)^{2/3} (1/R_i)^{1/3} \qquad (1).$$

Here E* is the composed (indenter/material) elastic modulus

$$1/E^* = (1-\nu_m^2)/E_m + (1-\nu_i^2)/E_i \qquad (2),$$

where ν_m and E_m are Poisson's ratio and the elastic modulus of the material, ν_i and E_i are Poisson's ratio and the elastic modulus of the indenter.

The mean pressure ($P_m = F/A$, where A is the area of contact) over the elastic footprint increases with the loading force until it reaches a limiting value set by yield stress of the undeformed material. From this point on, any increase in the load is accompanied by plastic yielding to limit the mean pressure to a value consistent with the yield stress of the deforming material. A plastic zone forms beneath the indenter, and after unloading a residual impression is left in the surface. The total depth of penetration (h_t) is then a sum of the elastic (h_e) and plastic (h_p) components, as it is illustrated also in Figs.1 and 2:

$$h_t = h_e + h_p \qquad (3).$$

Assuming that the elastic deformation is equally distributed above and below the circle of contact, the depth of penetration in contact (h_c) which also contains plastic and elastic components, is given as [1]

$$h_c = h_t – h_e/2 \qquad (4).$$

The radius of the circle of contact (a) is then given by geometry as

$$a^2 = 2R_ih_c – h_c^2 \qquad (5).$$

Because unloading in quasi-static regime is entirely elastic, the unloading curve can be analysed using Hertzian elastic contact mechanics and the Equation (1) becomes

$$h_e = (9/16)^{1/3} (F/E^*)^{2/3} (1/R_i – 1/R_m)^{1/3} \qquad (6),$$

where R_m is the curvature radius of the residual spherical depression, which can be found as

$$R_m = (a^2+h_p^2) / 2h_p \qquad (7).$$

The elastic modulus can be calculated directly from the unloading curve.

The critical stress condition, where a transition from elastic to elastic/plastic behaviour occurs, exists when the mean pressure equals the hardness of the tested surface. Therefore, at loads above the critical value, the hardness can be calculated as

$$H = F / \pi a^2 \qquad (8).$$

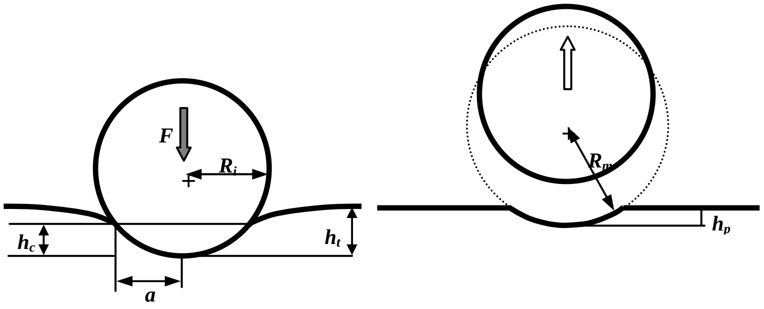

Fig.1. Schematic illustration of indentation of flat surface by spherical indenter.

Berkovich indenter

Berkovich indenter is a pyramid with the base of an equilateral triangle and 13.0° angle between the base and the edges (Fig.3). The hardness can be calculated from the depth of penetration (h) as

$$H = F / A = F / 24.5\, h^2 \qquad (9).$$

Using the depth sensing technique the modulus of elasticity can be found from Sneddon's equation for generalized parabolic/conical indenters [5]:

$$1/E^* \, dF/dh = 2\,(A/\pi)^{1/2} \qquad (10),$$

where dF/dh is the initial slope of unloading part of the load-depth curve, as it is illustrated in Fig.2.

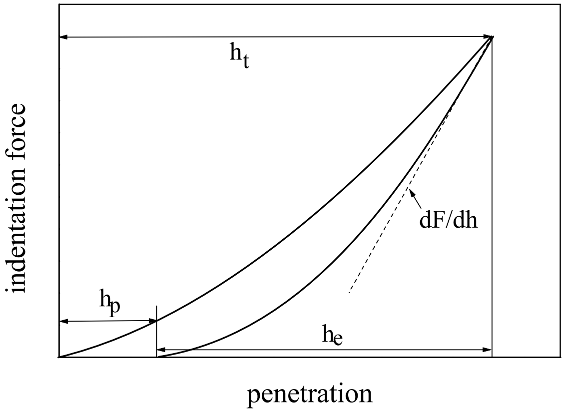

Fig.2. Separation of the components of penetration measured using DST. dF/dh is the slope used for calculation of Young's modulus.

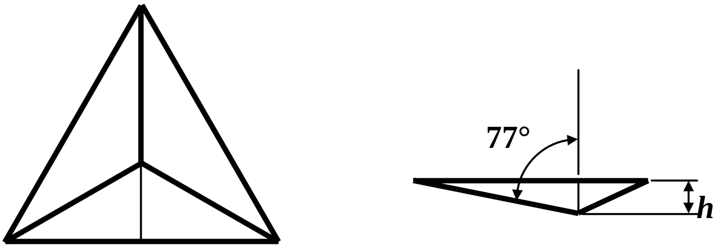

Fig.3. Geometry of Berkovich pyramid indenter. Top and side view.

EXPERIMENTAL MATERIAL

The material was prepared by densification of a Si_3N_4 / Y_2O_3 / C / SiO_2 starting mixture with weight fractions of 93.23% / 4.91% / 0.43% / 1.43 %, respectively. Green discs were then embedded into a BN powder bed and positioned into the graphite uniaxial die. Samples were hot-pressed under a specific heating regime, an atmosphere and mechanical pressure regime at 1750 °C and 30 MPa for 2 h. The SiC crystalline grains formed within the final composite. The details of fabrication and microstucture studies were published elsewhere [2]. For the indentation studies a piece with dimensions of 3x4x4 mm was used. Its surface was polished to a 0.25 μm final finish.

EXPERIMENTAL METHODS

The nanoindentation tests, using the depth sensing technique (DST), were carried out on UMIS 2000 (made by CSIRO Australia) ultramicroindentation system at room temperature in ambient air.

In the case of spherical indenter, the multiple partial unloading method developed by Field and Swain [6] and recently studied in detail by Bushby [1], was used. In this method, a single indentation is partially unloaded at each force step by a specific fraction (from 10 to 90%) of the load step. Each force step then provides two pieces of information: the total depth of elastic/plastic penetration, and a measure of the recovery from that load.

When the unloading part of the load cycle can be completely modelled analytically, such as the case of indentation with a sphere, two points at each load are sufficient to fully characterise unloading from each loading step. The residual unrecovered indentation depth (h_p), the elastic deflection of surface (h_e), and the depth below the circle of contact (h_c) were then calculated for each load step.

In the present study, a spherical diamond indenter with nominal radius $R_i = 7$ μm was used. Its modulus of elasticity was 1150 GPa and a Poisson's ratio 0.07. Loading force up to 300 mN in 30 incremental steps was applied, each step was followed by 25% unloading. Altogether, 20 tests were perfomed.

The modulus of elasticity of the material was calculated using an Equation (6) for each step's penetration depth, assuming $\nu_m = 0.2$ (value for Si_3N_4 [7]). The hardness was calculated from Equation (8) at loads from 270 to 300 mN which induced stresses well above the transition point. The partial unloading procedure also allows indentation stress-strain curves to be generated, where the mean pressure (P_m) is taken as indentation stress, and indentation strain is expressed as a ratio of a/R_i.

The hardness and modulus of elasticity were also measured by the Berkovich pyramid using simple loading-unloading method with a maximum applied force of 10 mN, which produced depths of penetration similar to those achieved at indentations with a 7 μm radius sphere.

The hardness was also measured independently by Vickers diamond indenter using Shimadzu Microhardness Tester. A series of 15 indents were made at 0.49 N, 0.98 N, 1.96 N, 2.94 N, 4.9 N, and 9.8 N. The Vickers hardness values were calculated from the lengths (d) of the imprint diagonals measured by an optical microscope as $HV = 1.8544\ F/d^2$.

RESULTS AND DISCUSSION

Figure 4 shows a typical result of the partial unloading test in the form of force-penetration data for extreme points at each step. When the material deforms elastically, the data for fully loaded and partially unloaded states lie on the same line. After exceeding the yielding point of the material, the recovery is no longer complete and two branches diverge. Each particular data pair lies on a curve equivalent to single loading-unloading, as it is illustrated in Fig.2 for the maximum load by the solid line.

The indentation stress-strain curves (Fig.5) obtained from the force-penetration data (Fig.4) show similar features to tensile or compressive stress strain curves. The initial portion is linear and corresponds to purely elastic deformation. The yielding point can be identified as the deviation from this elastic behaviour. In our tests these values ranged from 13.5 to 14.0 GPa, which is similar to the onset of plastic deformation for pure polycrystalline alumina (~ 14 GPa [1]). This information for ceramics and glasses is unique because conventional tensile or compressive tests normally result in catastrophic failure at much lower stresses.

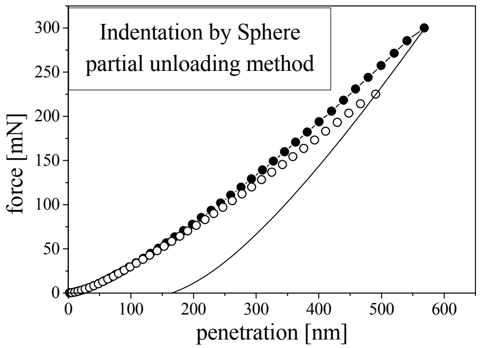

Fig.4. Force-penetration data from multiple partial unloading method: fully loaded (●) and partially unloaded (○) points.

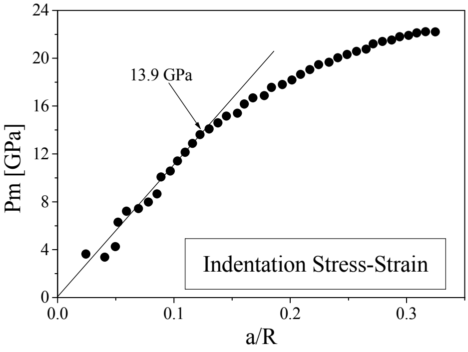

Fig.5. Indentation stress-strain curve for the Si_3N_4/SiC nanocomposite measured using multiple partial unloading method.

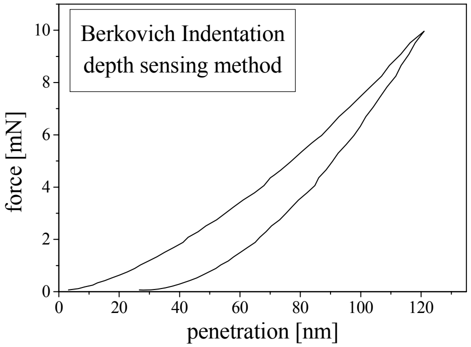

Fig.6. Loading – unloading curve of the Berkovich indentation.

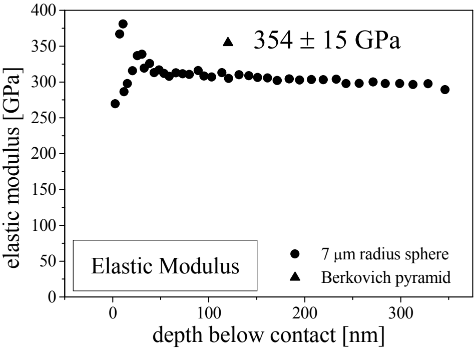

Fig.7. Modulus of elasticity measured by the depth sensing method of indentation.

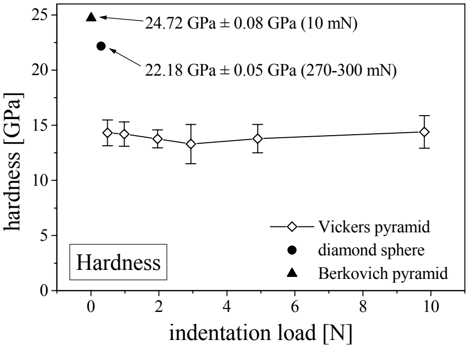

Fig.8. Comparison of the hardness values of the studied nanocomposite measured by different indentation techniques.

An example of the result of indentation with the Berkovich pyramid is shown in Fig.6.

Figure 7 shows values of modulus of elasticity calculated from the depth sensing indentation techniques. The average value obtained from indentation with a diamond sphere was 309 ± 20 GPa which is in good agreement with value for polycrystalline HPSN, 304 GPa [7]. The value for the composite can be estimated using the law of mixtures, $E = E_aV_a + E_bV_b$, where V_a and V_b are the volume fractions of the constituents. For our material with about 1% of SiC [2] with E from 414 to 440 GPa [7], this law gives E between 305 and 306 GPa. The indentation with the Berkovich pyramid gave 354 ± 15 GPa, which seems to be overestimated. This is probably caused by the non-ideal geometry of the indenter, which was not perfectly sharp. That means that the area of contact does not follow the square law with increasing depth of penetration precisely, particularly at very low loads and penetrations. The relatively large scatter of values of the elastic modulus measured by spherical indentation at very low loads (penetration depths < 15 nm) in Fig.7, is caused by errors in the reading of the depth which is, in these cases, close to the instrument resolution limits.

Figure 8 summarizes the hardness measurements. Both DST methods resulted in similar values, 22.18 GPa (sphere) and 24.72 GPa (Berkovich), that agree with the literature hardness data [7] for high density HPSN (22 GPa) with possible influence of SiC (27-33 GPa). As it can be seen, Vickers indentation gives generally lower values of hardness over a wide range of loads (~14.5 GPa). This can be partly due to the size of the stress field. Both DST methods were used at comparatively low loads. The sizes of areas of contact and also the stress fields were typically in the range of 0.1 to 3 μm, that is values comparable with the size of a single grain, which means that the influence of the porosity was negligible. On the other hand, the Vickers indentations produced large stress fields that included pores and all possible faults of the microstructure. However, the porosity of the material was less than 1% [2] and, therefore, it can not fully explain the low values of hardness. Other possible factors are then subjective error of the experimenter, and systematic error of the instrument, as this method relies on optical measurement of the indentation imprint size. The results of this method also typically exhibit a relatively large scatter.

CONCLUSION

The mechanical properties and deformation behaviour of Si_3N_4/SiC nanocomposite were investigated by indentation. Two different depth sensing methods and a standard hardness testing were used and corresponding results were compared. The depth-sensing methods provided reliable results, which were in very good agreement with the literature data, particularly in the case of well-defined spherical indenter. Indentation with the spherical indenter also enabled investigation of the elastic-to-elastic/plastic transition phenomena that are extremely difficult to study by using other methods. The Vickers indentation provided considerably lower hardness values. Its results were consistent over a wide range of indentation loads, but were more scattered and potentially most influenced by human error.

Acknowledgement

The UMIS measurements were performed at Queen Mary University of London. The financial support of the Slovak Grant Agency for Science via grant No. 2/1166/21 is gratefully acknowledged.

REFERENCES

[1] Bushby, A.J.: Nondestructive Testing and Evaluation, vol. 17, 2001, p. 213
[2] Šajgalík, P., Hnatko, M., Lenčéš, Z., Warbichler, P., Hofer, F.: Zeitschrift für Metallkunde, vol. 92, 2001, p. 937
[3] Hertz, H.: J. Reine Angewandte Math., vol. 92, 1882, p. 156
[4] Johnson, K.L.: Contact Mechnics, Cambridge University Press, London, 1985
[5] Sneddon, I.N.: Intl. Journal of Engineering Science, vol. 3, 1965, p. 47
[6] Field, J.S., Swain, M.V.: Journal of Material Research, vol. 8, 1993, p. 297
[7] Richerson, D.W.: Modern Ceramic Engineering, Marcel Dekker, New York, 1992